Journal of Alloys and Compounds 495 (2010) 88–92

Contents lists available at ScienceDirect

Journal of Alloys and Compounds

journal homepage: www.elsevier.com/locate/jallcom

Synthesis, formation mechanism and illuminated sensing properties of 3D WO_3 nanowall

Aihua Yan [a], Changsheng Xie [a,b,*], Dawen Zeng [b], Shuizhou Cai [b], Huayao Li [a]

[a] State Key Laboratory of Material Processing and Die & Mould Technology, Huazhong University of Science and Technology, 1037# Luoyu Road, Hongshan District, Wuhan 430074, China
[b] Nanomaterial and Smart Sensor Research Laboratory, Department of Materials Science and Engineering, Huazhong University of Science and Technology, 1037# Luoyu Road, Hongshan District, Wuhan 430070, China

ARTICLE INFO

Article history:
Received 18 November 2009
Received in revised form 17 January 2010
Accepted 19 January 2010
Available online 25 January 2010

Keywords:
Oxide materials
Chemical synthesis
Electronic properties
Light absorption and reflection

ABSTRACT

Three-dimensional WO_3 nanowall was successfully synthesized by a facile solvothermal approach in the solution of F127 template. The effect of solvent on tailoring morphology was investigated in detail. The results show that the products with a diameter of 1–3 μm are actually a kind of nanowall structure, which is composed of high-density nanosheets with about 30 nm in thickness. A possible formation mechanism is proposed here. Sensing properties show that the sensitivity of the three-dimensional WO_3 sensor is obviously higher than that of commercial WO_3 sensor. UV illumination on three-dimensional WO_3 sensor could greatly improve the response because of the formation of defects.

1. Introduction

It is well known that the physical and chemical properties of most materials are strongly dependent on their shape and structure. Therefore, controlling the shape of the materials is always one of the most challenging issues for inorganic chemists and material specialists. Recently, complex three-dimensional (3D) micro/nanoarchitectures have attracted substantial attention since such architectures combine the features of micrometer- and nanometer-scaled building blocks and provide a great deal of opportunity to explore their novel properties [1,2]. However, fabrication of more complex micro/nanoarchitectures and controlling the shape of nanostructures at the microscopic level are still a significantly challenging issue for material scientists.

As a kind of important material, nanometric tungsten oxide (WO_3) with a large surface-to-volume ratio has attracted considerable interests because of its special electronic and optoelectronic properties, which has enormous application potential in the fields of electrochromic materials [3], gas-sensing materials [4], electrocatalysts [5], lithium-ion batteries [6], optical storage media [7]. Current study of nanostructural tungsten oxide mainly focuses on 1D/2D structure with the aid of surfactants, such as nanowires [8], nanorods [9], nanosheets [10] and nanotips [11]. Due to the special properties of tungsten, it is hard to tune and control the morphology of WO_3, not to mention to organizing 1D/2D WO_3 nanostructure into well-defined 3D nanostructure. Blackman and his group found that 2D WO_3 nanostructure could be tuned through the change of the O-containing reactants, such as ethanoic anhydride, ethanol, methanol and water [12,13]. But further process mechanism was not explained. Moreover, to our best knowledge, there have no reports on assembly-controlled 3D WO_3 structure prepared by a simple surfactant-assisted method. Therefore, it is essential to further investigate the influence of O-containing solvents and other factors on the morphology in order to organize 1D/2D WO_3 structure into 3D WO_3 structure.

On the other hand, WO_3-based gas sensors have been widely used to detect NO_2, ethanol, and so on. However, high activation energy of reaction with gas molecules results in high work temperature, slow response time and recovery time, which restricts its further application in some specific environment. Since Saura et al. reported that the gas-sensing properties of SnO_2 films under UV radiation could markedly increase the desorption of oxygen species and conductivity [14], illuminating sensors to activate chemical reactions were widely investigated, especially, SnO_2-based, ZnO-based, In_2O_3-based, *etc.* [15–17]. However, few reports about WO_3 sensors under UV radiation were investigated.

Herein, we demonstrated a facile surfactant-assisted solvothermal method to synthesize 3D WO_3 nanowall based on nanosheet structure. Current study was initiated with the objectives of (1) fabricating controllable complex 3D WO_3 micro/nanomaterials, (2)

* Corresponding author. Tel.: +86 27 87556544.
E-mail address: csxie@mail.hust.edu.cn (C. Xie).

0925-8388/$ – see front matter © 2010 Elsevier B.V. All rights reserved.
doi:10.1016/j.jallcom.2010.01.092

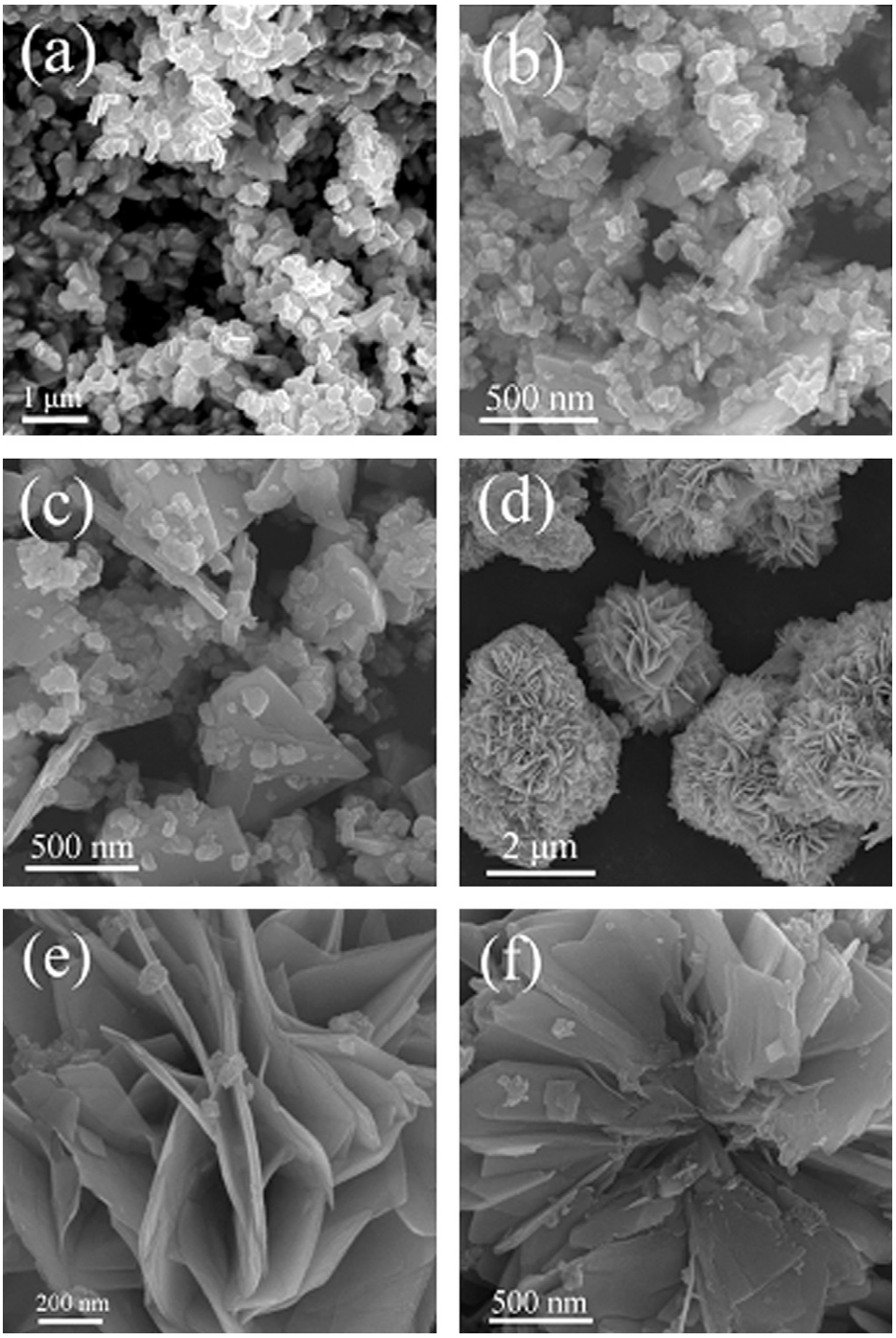

Fig. 1. FESEM images of the as-synthesized samples using different amounts of ethanol solvent: (a) 0%; (b) 20%; (c) 50%; (d), (e) and (f) 100%.

investigating the influence of different solvents and process conditions on the morphology, (3) analyzing the formation mechanism, and (4) insighting the relation between morphology and sensing properties under UV illumination.

2. Experimental procedures

2.1. Synthesis of the samples

All the chemicals were of analytic grade and used without further purification. In a typical procedure, 2 g pluronic F127 (Aldrich–Sigma Inc., American) was dissolved in deionized water. Then 2 g WCl_6 (Alfa Aesar Co., American) was added into above solution (70 mL) and stirred for 3 h. Then the mixed solution was transferred to a 80 mL teflon-lined autoclave. Subsequently, the autoclave was sealed and maintained at 120 °C for 24 h, following natural cooling to room temperature. Afterwards, the products were centrifugated and washed with deionized water and absolute ethanol for several times, respectively. The as-synthesized products were dried at 80 °C for 12 h and heat-treated at 550 °C for 3 h to remove the surfactant completely. In order to investigate the influence of solvent, different amounts of anhydrous ethanol were used to replace the water solvent.

2.2. Structural characterization

The morphologies and structures of WO_3 products were investigated by field emission scanning electron microscopy (FESEM, Hitachi S-4800, Japan). The composition and phase of the products were analyzed by X-ray diffraction (XRD, Rigaku D/MAX-rB, Japan) with Cu Kα irradiation (λ = 0.154056 nm).

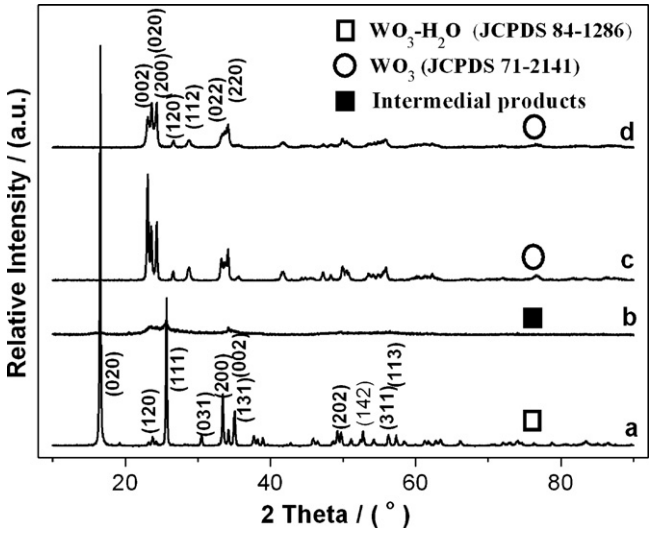

Fig. 2. XRD patterns of the samples synthesized under different conditions. (a) In water solvent before annealing; (b) in ethanol solvent before annealing; (c) in water solvent after annealing; (d) in ethanol solvent after annealing.

2.3. Sensing properties

The WO_3 gas-sensing sensors and testing methods were performed by static testing method [18]. Firstly, the above-synthesized WO_3 precursors were mixed with ethanol to form a paste. Then the paste was coated on the blank alumina tube with two platinum electrodes at each end. Subsequently, the dried thick films were treated at 550 °C for 3 h. The sensitivities of the films to nitrogen dioxide (NO_2) were investigated on a self-made static testing system. Before measurement, all tested samples were pre-stabilized at the working temperature for 3 days. During the testing, a given amount of saturated NO_2 gas was firstly injected into a storage chamber, and then carried into the testing chamber by air flow. Here the sensitivity (S) to the tested gas is defined as the ratio of R_g/R_a, where R_a and R_g are the resistances of the sensor in air and in the tested gas, respectively. The response time is defined as the time for a sensor to achieve 90% of the final voltage change due to the chemical adsorption.

3. Results and discussion

3.1. Influence of solvent on morphology

In hydrothermal/solvothermal reaction, solvent plays a key role in the composition and morphology of the final products. Recently, our group has systematically investigated the effect of solvent on the morphology of ZnO and found methanol additive could markedly change the morphology of final products [18]. Polleux, *etc*. found anhydrous benzyl alcohol could be used to synthesize homogeneous perovskite nanocrystal [19]. Blackman, *etc*. found that the O-containing reactants have great effect on the final films of WO_3 prepared by APCVD. The morphology was evolved from particle, needle, fiber, to sheet with the addition of ethanoic anhydride, ethanol, methanol and water [12,13]. Stucky and his group also found that tungsten oxide nanoplatelets could be synthesized using tungsten chloride and benzyl alcohol as raw materials [20].

To explore the exact role of solvent during the synthesis of WO_3 nanocrystals, we systematically changed the amount of H_2O through the replacement of anhydrous ethanol. The results demonstrate that the morphology of the products is greatly changed with the change of ethanol amount. Initially, the products synthesized in pure water solvent are particles with nearly square, "quasi" two-dimensional platelets structure (Fig. 1a). When 20% H_2O is replaced by the anhydrous ethanol, the main products still keep the same platelet structure. However, a small amount of products is evolved to nanosheets (Fig. 1b). With further replace of anhydrous ethanol to 50% H_2O, most products are evolved to sheetlike structure and only part of the products keeps platelet structure (Fig. 1c). Interestingly, when H_2O is fully replaced by anhydrous ethanol, all the products are evolved to complicated 3D nanowall structure with a diameter of 1–3 μm, which is composed of high-density nanosheets with about 30 nm in thickness, as shown in Fig. 1d and e. To further confirm the nanowall structure, the products were treated under strong ultrasonic wave for a long time. The results show all the nanosheets grow from the core and form the sector-like structure (Fig. 1f).

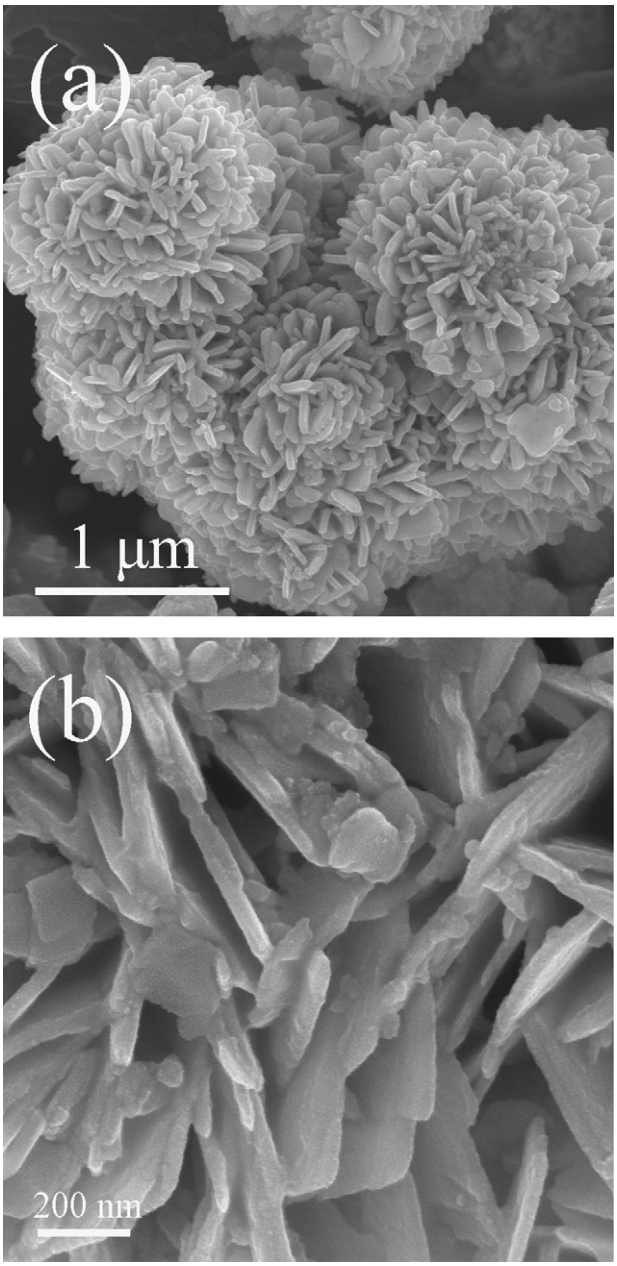

Fig. 3. SEM images of the 3D nanowall samples annealed at 550 °C.

Typical XRD patterns of the as-synthesized and final samples in water solvent and ethanol solvent are shown in Fig. 2. It is seen that all the diffraction peaks for the as-synthesized samples in water solvent can be indexed as orthorhombic $WO_3 \cdot H_2O$ (JCPDS 84-0886). While the diffraction peaks for the as-synthesized samples in ethanol solvent become wider and weaker. The possible reason may be attributed to organic species of ethanol and surfactant, which will be further explained in the following mechanism. After heat-treatment at 550 °C, all the samples synthesized in water solvent and ethanol solvent are converted to crystalline of mono-

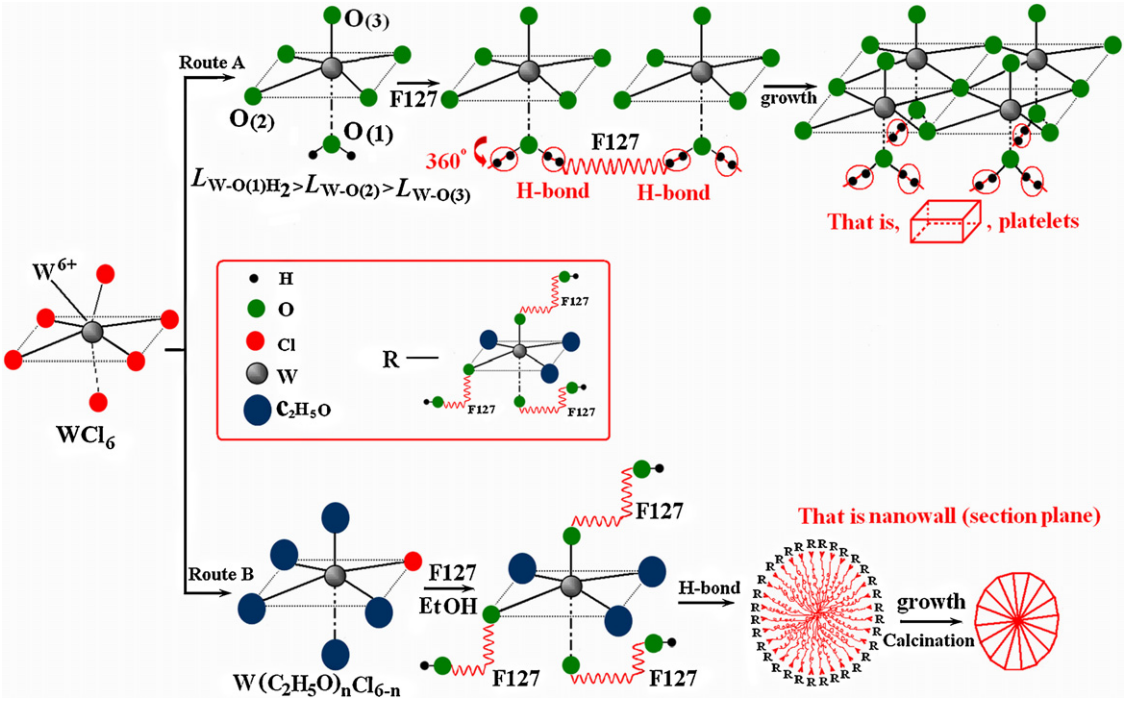

Fig. 4. Schematic diagram of process mechanism.

clinic WO_3, and no other characteristic peaks are detected. Fig. 3 shows the SEM images of the samples synthesized in ethanol solvent. It can be seen that the nanowall structure keeps unchanged after annealing.

3.2. Formation mechanism

Shen and his co-workers reported that WCl_6 hydrolyzes under a certain hydrothermal condition and gets $WO_3{\cdot}H_2O$ according to Eq. (1) and thought that $WO_3{\cdot}H_2O$ is formed of layers built up by corner sharing [WO_6] octahedral units, in which each tungsten atom is coordinated by five oxygen atoms and a water molecule [21]. Choi and his group found that only WO_3 nanoparticles were present when ethanol and water solvents were used as solvents without surfactant, indicating that surfactant is very important for the morphology evolution [22].

According to previous works and above experimental results, here we propose the growth model from the viewpoint of natural properties of tungsten to explain 3D WO_3 growth mechanism. The formation process of 3D WO_3 hierarchical nanostructure is illustrated in Fig. 4. Firstly, WCl_6 dissolves in water solvent and forms $WO_3{\cdot}H_2O$ sol. When F127 is used as structure-directing agent, the hydroxyl group of $WO_3{\cdot}H_2O$ and hydroxyl group of F127 will interact through H-bond and assist the $WO_3{\cdot}H_2O$ to grow along different directions in a given plane so long as the reaction is controlled in a certain condition, in another word, F127 induces the formation of $WO_3{\cdot}H_2O$ platelets through sixfold coordinated W^{6+} and subsequent oxolation action. When the mass of $WO_3{\cdot}H_2O$ arrives at a certain value, it tends to precipitate under a certain pressure. Consequently, $WO_3{\cdot}H_2O$ with two-dimensional platelets structure can be gained.

In aqueous solvent:

$$WCl_6 + 4H_2O = WO_3{\cdot}H_2O + 6HCl \quad (1)$$

In ethanol solvent:

$$WCl_6 + nC_2H_5OH = W(C_2H_5O)_nCl_{6-n} + nHCl \quad (2)$$

$$W(C_2H_5O)_nCl_{6-n} + (6-n)(Pr.) = W(C_2H_5O)_n(Pr.)_{6-n} + (6-n)HCl \quad (3)$$

(Here Pr. represents F127).

However, the reaction in anhydrous ethanol is slightly different from the reaction in water solvent. Djaoued and his co-workers reported the reaction mechanism of WCl_6 in anhydrous ethanol and thought that the overall reaction can be described according to Eq. (2) [23]. It should be stressed that a part of W^{6+} is reduced to W^{5+} in ethanol solvent, which can be indicated by the color change of the solution. Here the reducing reaction can be reduced to minimum through aging and heat-treatment for a long time. Here we thought that F127 block copolymer with hydroxyl can also react with $W(C_2H_5O)_nCl_{6-n}$ and replace other unreacted chlorine according to Eq. (3). In a word, the intermediated products include a large amount of F127 species which residual hydroxyl can induce the congregated growth through H-bond along different directions. After aging and growth for a long time, the final product could be nanowall structure. This model is in well agreement with XRD results because XRD pattern of as-synthesized 3D WO_3 is amorphous in nature compared to the as-synthesized samples in water solvent, which maybe result from large amount of F127 species.

After understanding the formation mechanism for 3D WO_3 in anhydrous ethanol solvent, it is not hard to understand the morphology evolution in mixed solvents. The key parameter is the reaction rate. Because the reaction rate of WCl_6 in water is faster than that in ethanol, the final morphology evolution is determined by water solvent, not by ethanol. Therefore, the products are mainly platelet and sheets, which is in well agreement with previous report [22].

3.3. Sensing properties

It is well known that morphologies of WO_3 nanostructures have great effect on sensing properties. Fig. 5 shows the relationship between the sensitivity to 500 ppb NO_2 and operating tempera-

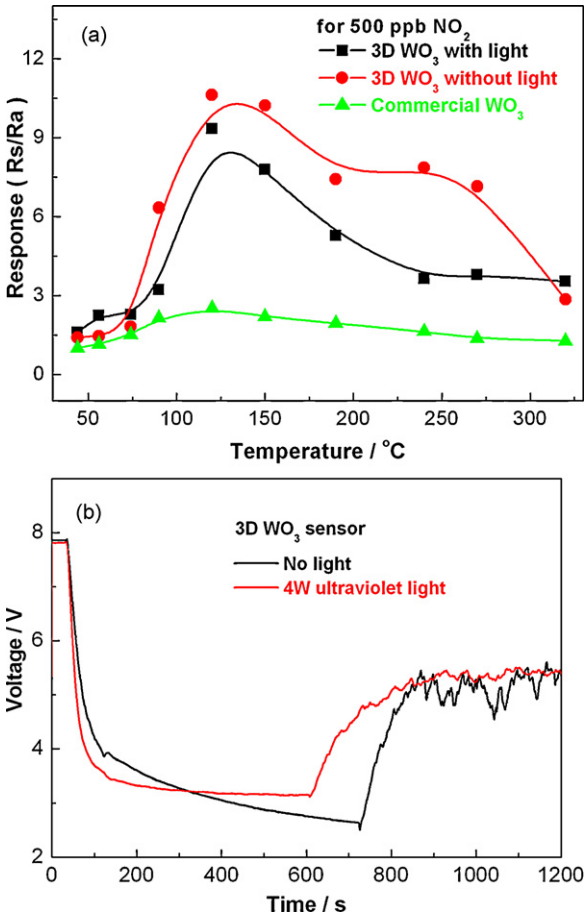

Fig. 5. Sensing properties of different samples to 500 ppb NO_2. (a) Sensitivity versus operating temperature curve; (b) response and recovery curve of the sample with and without light illumination.

ture. It can be seen that the sensitivity of all the samples increases with the increase of temperatures, then decreases above 120 °C. Compared to that of commercial WO_3, the sensitivity of 3D WO_3 sensors is obviously higher (Fig. 5a). The higher sensitivity of 3D WO_3 sensors is partly due to special 3D nano/microstructure, which could enhance the adsorption ability for NO_2 gas. Therefore, there are more electrons transferring from NO_2 to the sensing materials when a uniform coverage of the gases covers on the sensing layer. However, the sensitivity of 3D WO_3 with UV illumination is slightly lower than that without UV illumination. According to the definition of response time, it can be calculated that the response time of 3D WO_3 sensors with illumination and without illumination to 500 ppb NO_2 gas at 120 °C are 83.2 s and 370.1 s, indicating that UV light could greatly improve the response (Fig. 5b). The reason may be attributed to the formation of defects under UV illumination. In other word, illumination results in formation of vacancy by electrons and holes and activates chemical reactions on WO_3 surface, which could accelerate the recombination of vacancy with the electrons from the NO_2^- states. Consequently, it significantly changes concentration of the adsorption centers and the capacity of the adsorption on the surface. Therefore, the sensitivity could slightly decrease and the response could speed up.

4. Conclusions

In conclusion, 3D WO_3 nanowalls were successfully synthesized through controlling the amount of solvent. The results show that solvent has great effect on morphology evolution of WO_3 during the hydrothermal synthesis. The formation mechanism for 3D WO_3 is determined by the property and structure of tungsten in nature. The structural replacement of F127 determines its 3D growth in anhydrous ethanol solvent. Sensing properties of such WO_3 sensor show the desirable sensing characteristics towards 500 ppb NO_2 gas at 120 °C could obtain. UV illumination is an effective approach to achieve higher response for 3D WO_3 sensors.

Acknowledgements

This work was supported by the National Basic Research Program of China (Grant Nos. 2009CB939705 and 2009CB939702), Nature Science Foundation of China (No. 50927201) and the Opening Research Foundation of State Key Laboratory of Advanced Technology for Materials Synthesis and Processing (Wuhan University of Technology). The authors are also grateful to Analytical and Testing Center of Huazhong University of Science and Technology.

References

[1] F. Lu, W.P. Cai, Y.P. Zhang, Adv. Funct. Mater. 18 (2008) 1047–1056.
[2] B.X. Li, G.X. Rong, Y. Xie, L.F. Huang, C.Q. Feng, Inorg. Chem. 45 (2006) 6404–6410.
[3] S. Sallard, T. Brezesinski, B.M. Smarsly, J. Phys. Chem. C 111 (2007) 7200–7206.
[4] Y.S. Kim, S.C. Ha, K. Kim, H. Yang, S.Y. Choi, Y.T. Kim, J.T. Park, C.H. Lee, J.Y. Choi, J.S. Paek, K. Lee, Appl. Phys. Lett. 86 (2005) 213105.
[5] T. Arai, M. Yanagida, Y. Konishi, Y. Iwasaki, H. Sugihara, K. Sayama, J. Phys. Chem. C 111 (2007) 7574–7577.
[6] N.A. Galiote, F. Huguenin, J. Phys. Chem. C 111 (2007) 14911–14916.
[7] I. Turyan, U.O. Krasovec, B. Orel, T. Saraidorov, R. Reisfeld, D. Mandler, Adv. Mater. 12 (2000) 330–333.
[8] J. Polleux, A. Gurlo, N. Barsan, U. Weimar, M. Antonietti, M. Niederberger, Angew. Chem. Int. Ed. 45 (2006) 261–265.
[9] F.C. Cheong, B. Varghese, Y. Zhu, E.P.S. Tan, L. Dai, V.B.C. Tan, C.T. Lim, C.H. Sow, J. Phys. Chem. C 111 (2007) 17193–17199.
[10] Y. He, Y. Zhao, J. Phys. Chem. C 112 (2008) 61–68.
[11] J. Zhou, L. Gong, S.Z. Deng, J. Chen, J.C. She, N.S. Xu, R. Yang, Z.L. Wang, Appl. Phys. Lett. 87 (2005) 2231081–2231083.
[12] C.S. Blackman, I.P. Parkin, Chem. Mater. 17 (2005) 1583–1590.
[13] S. Ashraf, R. Binions, C.S. Blackman, I.P. Parkin, Polyhedron 26 (2007) 1493–1498.
[14] J. Saura, Sensor Actuat. B-Chem. 17 (1994) 211–214.
[15] F.R. Messias, B.A.V. Vega, L.V.A. Scalvi, J. Non-Cryst. Solids 247 (1999) 171–175.
[16] L. Peng, Q. Zhao, D. Wang, J. Zhai, P. Wang, S. Pang, T. Xie, Sensor Actuat. B-Chem. 136 (2009) 80–85.
[17] E. Comini, A. Cristalli, G. Faglia, G. Sberveglieri, Sensor Actuat. B-Chem. 65 (2000) 260–263.
[18] H.H. Wang, C.S. Xie, J. Cryst. Growth 291 (2006) 187–195.
[19] M. Niederberger, N. Pinna, J. Polleux, Angew. Chem. Int. Ed. 43 (2004) 2270–2273.
[20] M. Niederberger, M.H. Bartl, G.D. Stucky, J. Am. Chem. Soc. 124 (2002) 13642–13643.
[21] X.L. Wei, P.K. Shen, Electrochem. Commun. 8 (2006) 293–298.
[22] H.G. Choi, Y.H. Jung, D.K. Kim, J. Am. Ceram. Soc. 88 (2005) 1684–1686.
[23] Y. Djaoued, S. Priya, S. Balaji, J. Non-Cryst. Solids 354 (2008) 673–679.